HHS Public Access

Author manuscript

Neuroimage. Author manuscript; available in PMC 2016 July 15.

Published in final edited form as:

Neuroimage. 2015 July 15; 115: 76–84. doi:10.1016/j.neuroimage.2015.04.060.

Nature of Functional Links in Valuation Networks Differentiates Impulsive Behaviors between Abstinent Heroin-Dependent Subjects and Nondrug-Using Subjects

Tianye Zhai[1,2,3,*], **Yongcong Shao**[1,*], **Gang Chen**[2], **Enmao Ye**[1], **Lin Ma**[4], **Lubin Wang**[1], **Yu Lei**[1], **Guangyu Chen**[2], **Wenjun Li**[2], **Feng Zou**[1], **Xiao Jin**[1], **Shi-Jiang Li**[2,†], and **Zheng Yang**[1,†]

[1]Cognitive and Mental Health Research Center, Beijing Institute of Basic Medical Science, Beijing, P.R. China

[2]Department of Biophysics, Medical College of Wisconsin, Milwaukee, Wisconsin, USA

[3]Institute of Basic Medical Sciences, Chinese Academy of Medical Sciences, School of Basic Medicine, Peking Union Medical College, Beijing, P.R. China

[4]Department of Radiology, The General Hospital of the People's Liberation Army, Beijing, P.R. China

Abstract

Advanced neuroimaging studies have identified brain correlates of pathological impulsivity in a variety of neuropsychiatric disorders. However, whether and how these spatially separate and functionally integrated neural correlates collectively contribute to aberrant impulsive behaviors remains unclear. Building on recent progress in neuroeconomics towards determining a biological account of human behaviors, we employed resting-state functional MRI to characterize the nature of the links between these neural correlates and to investigate their impact on impulsivity. We demonstrated that through functional connectivity with the ventral medial prefrontal cortex, the δ-network (regions of the executive control system, such as the dorsolateral prefrontal cortex) and the β-network (regions of the reward system involved in the mesocorticolimbic pathway), jointly influence impulsivity measured by the Barratt Impulsiveness Scale scores. In control nondrug-using subjects, the functional link between the β- and δ-networks is balanced, and the δ-network competitively controls impulsivity. However, in abstinent heroin-dependent subjects, the link is

[†]Corresponding Authors: Zheng Yang, MD, PhD, Beijing Institute of Basic Medical Science, 27 Taiping Road, Beijing, PR China, Tel.: +86 10 68210161; Fax: +86 10 68210161., Yangzhengchina@aliyun.com. Shi-Jiang Li, PhD, Department of Biophysics, Medical College of Wisconsin, 8701 Watertown Plank Road, Milwaukee, Wis. 53226 USA, Tel: 414-955-4029; Fax: 414-955-6512, sjli@mcw.edu.

[*]These authors contributed to this manuscript equally.

Disclosure

All authors have made substantial intellectual and physical contributions to this paper in one or more of the following areas: design or conceptualization of the study, data acquisition, data analysis and interpretation, drafting and revising the manuscript. All authors have given final approval of this manuscript. None of the authors of this paper have reported any possible conflict of interest, financial or otherwise, related directly or indirectly to this work.

imbalanced, with stronger β-network connectivity and weaker δ-network connectivity. The imbalanced link is associated with impulsivity, indicating that the β- and δ-networks may mutually reinforce each other in abstinent heroin-dependent subjects. These findings of an aberrant link between the β- and δ-networks in abstinent heroin-dependent subjects may shed light on the mechanism of aberrant behaviors of drug addiction and may serve as an endophenotype to mark individual subjects' self-control capacity.

Keywords

neuroeconomics; valuation networks; resting-state functional connectivity MRI; heroin addiction; self-control

Introduction

Aberrant behaviors related to impaired self-control have been observed in a variety of neuropsychiatric disorders, including substance addiction (Baler and Volkow, 2006), pathological gambling (Limbrick-Oldfield et al., 2013), and ADHD (Sonuga-Barke and Fairchild, 2012). Advanced neuroimaging studies identifying brain correlates of impulsivity may provide insights into the nature of these aberrant self-control behaviors. Interestingly, the brain correlates underlying these disorders bear striking similarities. For example, it is well documented that drug addicts, pathological gamblers and ADHD subjects exhibit high impulsivity reflected by steep value discounting. This elevated impulsivity is usually correlated with weak top-down executive neural networks (including brain regions such as the DLPFC), and with hypersensitive reward networks (including brain regions such as OFC, dorsal striatum, thalamus, vmPFC, and NAcc) (Lawrence et al., 2009; Limbrick-Oldfield et al., 2013; Peters and Büchel, 2011; Sonuga-Barke and Fairchild, 2012). Obesity also shows significant functional abnormalities in discrete brain regions, especially in the ventral and dorsal striatal networks (Volkow et al., 2012; Tomasi and Volkow, 2013). Similar to the above findings, Shannon et al. demonstrated that the functional connectivity of the default mode and attention/control networks may predict juvenile offenders' impulsivity (Shannon et al., 2011). These converging results strongly suggest that many aberrant behaviors that are associated with impaired self-control may be supported by competing interactions between the reward networks and the executive control networks (Bechara, 2005; Bickel et al., 2007; Monterosso and Piray, 2012; Peters and Büchel, 2011).

However, less is known about the competing mechanisms among these networks. In particular, it is not well understood how these regionally separate yet functionally integrated brain correlates interact, and how these interactions further result in aberrant behavioral manifestations. Previous studies demonstrated that, in a single-valuation network model, the major regions of the valuation network were the vmPFC, OFC, and striatum (Kable and Glimcher, 2007, 2009). In contrast to the single-valuation network model, McClure et al. proposed a dual-valuation network model (McClure et al., 2007; McClure et al., 2004). In this model, the valuation network is defined as a "β-network" for mediating the short-term or immediate value, whereas the executive control systems are defined as a "δ-network", which modifies the long-term value. Hare *et al.* proposed a self-control model (Hare et al.,

2009) and more research results suggested that the executive control system (involving the DLPFC and parietal cortex) modulates the valuation network (including the OFC, striatum, thalamus and vmPFC) (Bartra et al., 2013; Baumgartner et al., 2011; Figner et al., 2010; Peters and Büchel, 2011; Steinbeis et al., 2012). These studies advanced the single- and dual-valuation models and suggested that although the β- and δ-valuation networks are spatially separate and functionally distinct, they are integrated to determine valuation. Nevertheless, the question remains as to why the δ-network, when confronted with a decision or choice, can exert its modulating function over the β-network in healthy people, but not in subjects with aberrant self-control behaviors. Indeed, it is simply not clear how the β- and δ-valuation networks are linked to bias the preference in individuals with aberrant self-control behavior.

This study assessed these valuation networks using resting-state functional MRI with the vmPFC as a connective node or a “seed” region. The selection of the seed region is based on the critical functions of vmPFC in the valuation network. The vmPFC plays a significant role in encoding and integrating subjective value signals, in assigning and optimizing decision-making processes, and in coordinating and evaluating the significance of alternative rewards (Bartra et al., 2013; Grabenhorst et al., 2011; Hare et al., 2010; Hare et al., 2009; Kable and Glimcher, 2007, 2009). We focused on characterizing β- and δ-network features and on investigating the nature of their links in heroin-dependent (HD) and control nondrug-using (CN) subjects to test our hypothesis that alterations exist in the natural links between the β- and δ-networks in heroin addiction, and that these alterations are associated with exhibited impulsivity.

Materials and methods

Participants

Thirty abstinent HD subjects were recruited from Beijing Ankang Hospital (Beijing, China), and 20 CN subjects also participated in this study. Both participant groups consisted of right-handed males, of normal intelligence, who were well-matched for age and years of education. Inclusion and exclusion criteria for heroin abusers and control subjects were described previously (Fu et al., 2008). In summary, each HD subject met DSM-IV criteria for heroin dependence, used heroin for more than two years, and was abstinent for at least two weeks. They also tested negative for morphine through urinalysis and negative for HIV in a blood test. None of the subjects had a history of neurological or psychiatric diseases, seizures, or head injury. None of the subjects were shown to have other structural abnormalities by an anatomical MRI scan. Two experienced psychiatrists assessed the inclusion and exclusion process, in accordance with the SCID. The study was approved by the Research Ethics Committee of Beijing Ankang Hospital and Beijing Institute of Basic Medical Science. The entire experiment was conducted in accordance with the Declaration of Helsinki. Written informed consent was obtained from all individual subjects prior to the study. Eight HD and five CN subjects were excluded from this study due to excessive motion artifacts (i.e., translational movement exceeded 1 mm or more than 1° rotational movement), thus leaving 22 and 15 subjects in the HD and CN groups, respectively, for further analysis.

Behavioral Measurement

The BIS-11 (Chinese version) was employed to assess study subjects' impulsivity (Patton et al., 1995). The BIS-11 has 30 4-point Likert-type items, which provide an overall total score and three subscale scores for Attention, Motor and Nonplanning impulsiveness. Higher scores signify higher impulsivity.

MRI Acquisition

MR images were acquired by a 3T Signa GE scanner with a standard quadrature transmit and receive head coil. The whole-brain resting-state fMRI data was acquired with a single-shot gradient-recalled EPI sequence, and the scanning parameters were as follows: TE of 25 ms, TR of 2 sec, flip angle of 90°, 20 slices, slice thickness of 5 mm (with an additional 1-mm gap space), imaging matrix size of 64 × 64, FOV of 24 cm × 24 cm. All 180 time points of images were collected in 6-minute resting scans without task performance. All subjects were instructed to not fall asleep, keep their heads still, and close their eyes. We also acquired high-resolution anatomical images of each individual subject, using a T1-weighted 3D-SPGR pulse sequence with the following scanning parameters: TE of 4.8 ms, TR of 10.4 ms, flip angle of 15°, 140 slices without spacing, slice thickness of 1 mm, matrix size of 256 × 256, FOV of 24 cm × 24 cm. In addition, we also recorded each subject's cardiac and respiratory signals for physiological noise corrections during image preprocessing.

Image Preprocessing

All imaging data preprocessing and functional synchrony analyses were conducted using the AFNI software (http://afni.nimh.nih.gov/afni/), and the SPM8 package (http://www.fil.ion.ucl.ac.uk/spm/software/spm8/) on Matlab platform. For imaging preprocessing, the first five dataset volumes were discarded due to the T1 nonequilibrium effect, then slice timing correction and volume registration (*3dvolreg, AFNI*), linear detrend (*3dDetrend, AFNI*), and physiological noise correction for respiratory and cardiac signals (*3dretroicor* and *3dDeconvolve, AFNI*) were performed. Also, noise from WM, CSF, global signal and six-way motion vectors was regressed out (*3dDeconvolve, AFNI*). A band-pass filter was then applied to keep the low-frequency fluctuations between 0.015Hz and 0.1 Hz (*3dFourier, AFNI*) (Fox and Raichle, 2007; Fransson, 2005).

Statistical Analysis

Structural Image Analysis—An o-VBM analysis was conducted using SPM8 (Good et al., 2001) to calculate the GM volume of subjects within each group. All subjects' individual T1-weighted 3D-SPGR images were first segmented into three parts — GM, WM, and CSF. The segmented GM was then normalized into MNI space. Meanwhile, the anatomical images were also normalized into MNI space, using the deformation field generated by the normalization of GM. The normalized anatomical images were then segmented for the second time and smoothed with an 8-mm FWHM Gaussian kernel. The o-VBM procedure was completed and the current segmented (second time) GM (modulated images) could be extracted to determine each individual's GM volume using a cluster detection method (*3dclust, AFNI, cluster detection size set as voxel size = 2 mm × 2 mm × 2 mm*). Each

individual's GM volume was further used as a covariate of no interest when conducting the ANCOVA test, as described below.

The vmPFC functional network maps using the seed-based method—The widely-employed, seed-based functional connectivity analysis has been reviewed extensively (Biswal et al., 1995; Fox and Raichle, 2007). Specifically, the predefined bilateral vmPFC regions, as ROIs that were centered on the Talairach coordinates (x, y, z) of [−6, 48, −6] for the left vmPFC and [6, 48, −6] for the right vmPFC, were selected spherically with a 6-mm radius (*3dcalc*, AFNI) in accordance with previous literature (Bartra et al., 2013; Grabenhorst et al., 2010). The seed vmPFC regions were transformed onto each individual's original image space with reference to his anatomical images (*3dfractionize, AFNI*). Only voxels in EPI functional images that occupied more than 70% of the masked anatomical images in the resampled ROI masks were included in the voxelwise analysis (Zhai et al., 2014). For each individual, the averaged time courses within the seed ROIs were then extracted from the preprocessed EPI functional images and correlated with whole-brain voxel time courses using Pearson CC. Two CC maps (the left- and right- vmPFC CC maps) were calculated for each individual subject. The CC maps were converted to *z* maps with r-to-z transformation [$z = 0.5*\ln(1+r)/(1-r)$]. Each individual's z maps were then spatially normalized to the Talairach template, resampled to 2-mm isotropic voxels, and smoothed with a 6-mm Gaussian kernel, resulting in two normalized z-maps (the left- and right- vmPFC z-maps). One-sample *t*-tests were conducted to obtain the group-level functional connectivity patterns for both the left- and the right- vmPFC, using the normalized left- and right- z-maps of each individual as input data, with voxelwise significance level $p < 0.05$, and corrected for multiple comparison using the Alphasim method.

Group difference in vmPFC functional connectivity strength—In order to determine the difference in vmPFC functional connectivity strength between HD and CN groups, a voxelwise ANCOVA was conducted, based on the normalized z-maps across all subjects (*3dRegAna, AFNI*). The factors, such as each individual's left and right vmPFC side', age, years of education and GM volume, were regressed out from the main group effects as covariates of no interest. The difference map in the vmPFC functional connectivity was obtained with the familywise multiple comparison correction method (*3dClustSim, AFNI, α=0.025*, $p < 0.05$, cluster size > 6808 mm^3).

To quantitatively assess the nature of the link between the β- and δ-networks through the vmPFC, we converted the voxelwise difference map of regional FC strengths in the β- and δ-network regions into a composite numerical index and defined it as the β-index or δ-index, respectively. The predefined β- and δ-network regions were selected in the Talairach space, in accordance with previous research reports (McClure et al., 2007; McClure et al., 2004). The bilateral precuneus, nucleus accumbens, caudate, putamen, medial OFC, thalamus, and PCC were selected for the β-network regions, and the bilateral DMPFC, DLPFC, right IFG, and right IPL were selected for the δ-network regions. The conjunction analysis was conducted between the FC difference map and the predefined β- and δ-network regions. The z values in the overlapping voxels were averaged within the β-network regions for each

individual subject (βi), and then grouped for the CN and HD subjects. A similar calculation was conducted within the δ-networks. We further measured the difference between the β- and δ-index. For each individual subject, the difference in connectivity strength between the β- and δ-networks was calculated as the ($\delta_i - \beta_i$) index, where δ_i and β_i represented indices for the i^{th} individual subject.

Neural correlates of impulsivity measured by BIS scores in HD and CN groups—To understand the behavioral significance of HD subjects' imbalanced β- and δ-network strengths, a voxelwise multivariate linear regression analysis was conducted (*3dRegAna, AFNI*) between the individual z-map and the measured BIS total score (and also between the individual z-map and the three subscores of BIS). This analysis was conducted for the HD group and the CN group, respectively, to avoid group effects. In the same manner as noted previously, each subject's factors, such as side,' age, years of education, and GM volume were controlled as covariates of no interest. The neural correlates maps also were corrected for multiple comparisons (*3dClustSim, AFNI, α=0.025, p* <0.05, cluster size > 6060mm^3).

The relationship between the impulsivity and the β- and δ-network activity—To test whether the spatially segregated β- and δ-networks are functionally integrated to predict the impulsivity of each individual in the HD and CN groups, we utilized multivariate linear regression analyses between the β- and δ-network indices and the measured impulsivity values, using the following fitting model:

$$BIS = \alpha_0 + \alpha_1 \beta + \alpha_2 \delta + \varepsilon$$

To obtain the *β- and δ-index*, we first calculated the union of neural correlate maps between the HD and the CN groups. The union maps then underwent conjunction analysis with the group difference map in functional connectivity and the predefined β- and δ-network regions (McClure et al., 2007; McClure et al., 2004). From the conjunction analysis results, we obtained both the β-network mask and the δ-network mask. Second, we averaged the z values within the β-network mask across subjects to determine the β-index. Similarly, we averaged the z values within the δ-network mask to determine the δ-index across subjects. Third, we utilized multivariate linear regression analyses, using the above-mentioned model. The regression analyses were conducted for two separate subject groups. The three dimensional results were projected onto the β- and δ-network axis, respectively, to obtain two-dimensional presentation. The factors of age, years of education, and GM volume of each individual were regressed out in all abovementioned regression analyses. Finally, we applied the LOO method to cross-validate the regression analysis results (Theodoridis and Koutroumbas, 2006). We applied these procedures to predict the relationships between the β- and δ-network connectivity strength and the BIS total score, as well as its subscores of Attention, Motor, and Nonplanning.

Results

Demographic information and behavioral measurement

Thirty-seven right-handed male volunteers, including 20 HD subjects and 15 CN subjects, were recruited. Table 1 outlines the study subjects' demographic information and characterization. No significant differences in age or years of education were evident when the HD and the CN groups were analyzed. The measured BIS-11 total score was significantly higher in HD subjects than in CN subjects ($p = 0.007$). Also, the BIS-11 subscale scores were higher in HD subjects than in CN subjects, ($p = 0.03$ for Attention, $p = 0.02$ for Motor and $p = 0.049$ for Nonplanning). The higher BIS-11 scores represented higher impulsivity in HD subjects relative to CN subjects. In addition, the o-VBM comparison also identified a decrease in GM volume in HD subjects compared with CN subjects ($p = 0.02$).

The patterns and group difference of vmPFC FC for the HD and CN group

Supplementary Fig. 1A illustrates the FC patterns of the left vmPFC (−6, 48, −6) for the CN group (left panel) and the HD group (right panel). Supplementary Fig. 1B shows the FC patterns of the right vmPFC (6, 48, −6) for the CN group (left panel) and the HD group (right panel). The voxelwise significance level of these two maps was set at the threshold of $p < 0.05$ (Alphasim corrected for multiple comparison).

Fig. 1A shows the difference map of the vmPFC functional network between the CN and HD subject groups, using the ANCOVA method. Specifically, we discovered that the FC strength between the vmPFC and the various β-network components including the bilateral caudate, NAcc, right medial OFC, right thalamus, and right PCC, was significantly increased in the HD group compared with the CN group. In contrast, the FC strength between the vmPFC and various δ-network components including the bilateral DMPFC, DLPFC, right IFG, and right IPL, was significantly decreased in the HD group compared with the CN group, as listed in Supplementary Table 1.

Figs. 1B and 1C illustrate that, in the HD group, the β-index is higher, whereas the δ-index is lower, in contrast to the CN group. As shown in Fig. 1D, the strong β-network activity overdrives the δ-network activity in HD subjects, resulting in a negative ($\delta_i - \beta_i$) value in most of the HD subjects, whereas most of CN subjects showed balanced FC (the $\delta_i - \beta_i$ is around zero). These results demonstrated that through the links to the vmPFC, the interaction between the β- and δ-networks was balanced in the CN group but imbalanced in the HD group. Further, the degree of the balance between the network connectivity ($\delta_i - \beta_i$) can be quantitatively measured and may be employed to index the neurophysiological deficit of HD subjects' self-control capacity.

The association between BIS total impulsivity and the FC strength of β- and δ-networks in HD subjects

We conducted two experiments to test whether β- and δ-network connectivity strengths correlate with individual subject impulsivity. First, we identified neural correlates between the measured BIS total score and the vmPFC FC in both the CN and HD groups, as shown in

Figs. 2A and 2B. Second, we conducted a conjunction analysis to obtain the overlapping regions among 1) the neural correlate impulsivity maps; 2) the FC group difference map as shown in Fig. 1A; and 3) the predefined regions involved in the β- and δ-networks (*see* **Methods**). The conjunction analysis maps are shown in Fig. 2C and listed in Table 2. These conjunction maps demonstrate that both β-network components (red) and δ-network components (green), rather than either one alone, are significantly associated with impulsivity.

We performed a multivariate linear regression analysis in which the BIS-11 total score served as a function of the variables of β- and δ-index (*see* **Methods**). The measured β- and δ-index of individual HD subjects and the corresponding impulsivity measured with the BIS-11 total score fit the model significantly ($F_{(2,19)} = 4.94$, p=0.019, $R^2 = 0.34$). Displaying plots into two dimensions, Fig. 2D shows that BIS-11 total score positively correlates with β-network connectivity ($F_{(1,20)} = 5.00$, p=0.037, $R^2 = 0.20$, left panel), and negatively correlates with the δ-network connectivity ($F_{(1,20)} = 9.34$, p=0.006, $R^2 = 0.32$, middle panel). In other words, an HD subject who has higher impulsivity would present stronger β-network FC strength and weaker δ-network FC strength. It appears that β-network and δ-network are mutually reinforced to tilt the network balance toward impulsive behaviors. In addition, the LOO cross-validation results are shown in Fig. 2D (right panel). The LOO method cross-validated the relationship and impulsivity may be predicted, according to β- and δ-network strength.

The association between Motor impulsivity and the FC strength of β- and δ-networks in HD subjects

The above conjunction analyses and the multivariate linear regression model were also performed with the BIS II Motor subscale of impulsivity. The results are shown in Supplementary Fig. 2 and Fig. 3A and listed in Table 3. The conjunction maps of the HD group demonstrate that both β- and δ-network components are significantly associated with subscale BIS II Motor impulsivity, rather than either the β- or δ-network alone. Individual subjects' calculated β- and δ-index and the corresponding impulsivity, as measured by BIS II Motor score, also fit the model significantly ($F_{(2,19)} = 6.72$, p=0.006, $R^2 = 0.41$). The plots are displayed in two dimensions, as shown in Fig. 3B. BIS II Motor impulsivity positively correlates with β-network FC strength ($F_{(1,20)} = 9.99$, p=0.005, $R^2 = 0.33$, left panel), and has a negative correlation with δ-network FC strength ($F_{(1,20)} = 11.00$, p=0.03, $R^2 = 0.35$, middle panel). This result is similar to that shown in Fig 2D. For other BIS subscales, there is no significant relationship with imbalanced β- and δ-network FC strength in HD subjects.

The association between Nonplanning impulsivity and the FC strength of β- and δ-networks in CN subjects

We also applied the above analyses to CN subjects, using the BIS total score of impulsivity and its three subscales. Only the BIS III Nonplanning impulsivity subscale was significantly fitted to the multivariate linear regression model ($F_{(2,12)} = 7.11$, p=0.009, $R^2 = 0.54$). Supplementary Fig. 3 shows the neural correlates of BIS III Nonplanning impulsivity in the CN (Supplementary Fig. 3A) and HD (Supplementary Fig. 3B) groups. Fig. 4A shows the conjunction map results, which are listed in Table 4. The δ-network components are

significantly associated with subscale BIS III Nonplanning impulsivity in the CN group. Compared with the above-mentioned HD group results, fewer β-network components (red color) were involved. The two-dimensional scatterplots from the multivariate linear regression model results show that although the β-network index does not significantly correlate with Nonplanning impulsivity ($F_{(1,13)} = 0.02$, p=0.87, $R^2 = 0.001$, left panel), the δ-network index is positively correlated with Nonplanning impulsivity ($F_{(1,13)} = 10.87$, p=0.006, $R^2 = 0.35$, middle panel (Fig. 4B). Nonplanning impulsivity seemed to be mediated by δ-network FC strength in CN subjects. The multivariate linear regression model was also cross-validated with the LOO method to predict that δ-network competitively mediates Nonplanning impulsivity (right panel).

Discussion

This study is primarily grounded in the neuroeconomic model, which indicates that the β- and δ-networks jointly influence neural processes in valuation, although they are spatially separate and functionally distinct (McClure et al., 2007; McClure et al., 2004). Traditionally, task-driven functional MRI studies characterized these network properties in a wide variety of control-demanding tasks. In contrast, resting-state functional MRI studies examine spontaneous activity between networks (Bullmore and Sporns, 2009; Fox and Raichle, 2007; Meehan and Bressler, 2012). In the functional connectivity literature, the β-network is generally referred to as the short-term reward network mediated by the mesocorticolimbic systems, while the δ-network is generally termed the “executive” or “control” network for long-term valuation properties mediated by the lateral prefrontal cortex and parietal cortex (McClure et al., 2007; Reuben et al., 2010; Sharp et al., 2012). It has been reported that, in normal subjects, resting-state functional connectivity may predict impulsivity in economic decision-making tests (Li et al., 2013). In addicted subjects, the FC patterns have been well characterized, and altered FC patterns were demonstrated in heroin- (Ma et al., 2010; Xie et al., 2011; Zhai et al., 2014) and cocaine-dependent subjects (Gu et al., 2010).

Despite these advancements, however, scientists and clinicians remain puzzled by the question why CN subjects can control their impulsivity in terms of resisting drugs, while HD subjects cannot. Previous studies proposed a competitive neural mechanism between the δ-network and the β-network (Bechara, 2005; Bickel et al., 2007). In testing this mechanism, there are two challenges. One is the methodological issue of how to establish the links between the β- and δ-networks to test whether they are balanced. The other challenge is the conceptual framework related to the duality of valuation networks. It is unclear whether the impulsivity is jointly determined by the δ-network and the β-network, or by the β-network alone.

In order to tackle the methodological challenge, we employed iBOLD signals measured by resting-state functional MRI methods to construct the neural network (Auer, 2008; Biswal et al., 1995; Engel et al., 2001; Fox and Raichle, 2007; Fransson, 2005; Greicius, 2003; Li et al., 2002). Compared with task-driven functional MRI methods, the resting-state functional MRI-based functional connectivity maps proved to be similar to task-induced activation maps, and they provide connectivity patterns measured by the synchrony of iBOLD signals among spatially distributed brain regions (Fair et al., 2007; Fox and Raichle, 2007). Our

current study is just building on the advancements of this large-scale brain network characterization and also on our current understanding of structure-function relationships (Park and Friston, 2013). We used vmPFC as a seed region to generate the vmPFC FC maps because it plays a central role in the valuation function (Bartra et al., 2013). We discovered that the β- and δ-network components are linked with the vmPFC, and there were significant differences between the CN and HD groups. This approach helped us to establish links between the β- and δ-networks, thereby allowing us to study their interactions. Such an approach is not based on the traditional task-driven functional MRI method, which tests ongoing stimulus-response activity. Rather, it is based on the iBOLD signals reflecting different aspects of intrinsic brain functional organization.

With regard to the conceptual duality framework of valuation networks, the present study demonstrated that β- and δ-networks jointly influence neural processes in valuation. There is an ongoing debate about valuation models, which are the single, dual, and self-control models (Hare et al., 2009; Kable and Glimcher, 2007; McClure et al., 2007; McClure et al., 2004). Our findings indicate that the interactive link between the β- and δ-networks might mutually modulate behavioral impulsivity. This strongly suggests that decision-making processes and impulsive behaviors not only depend on the δ-network for top-down control (Dalley et al., 2011), but also rely on the β-network for bottom-up drive. We believe our findings have implications for understanding aberrant behaviors and the manner in which the β- and δ-networks interactively regulate conflicting decision-making processes.

Our results corroborate earlier findings and also extend them in three important ways. First, it was suggested that β- and δ-network might engage in competing processes (Bickel et al., 2007). According to the competing account, subjects with strong impulsivity would have strong δ-network FC strength (executive control) to competitively balance motivational drive. Our CN subject results support the competing hypothesis. We demonstrated that the β- and δ-network FC strength of our CN subjects are in balance (i.e., $\delta_i - \beta_i$ value is around zero). In addition, the FC strength of δ-network positively correlated with Nonplanning impulsivity, indicating in the case of stronger impulsivity, there is stronger δ-network FC strength, implicating the influence of executive control over impulsive behavior. In contrast, in HD subjects, the δ-network FC strength was negatively correlated with impulsivity. The stronger the impulsivity was, the weaker the δ-network FC strength. The δ-network surrendered its ability to competitively balance the β-network. As a result, the weaker δ-network FC strength, coupled with stronger β-network FC strength, implicated the mutually reinforcing pattern to synergistically tilt the network balance toward motivational drive and lead to impulsive behaviors (i.e., $\delta_i - \beta_i$ value is negative). It has been suggested that this imbalanced neural mechanism may be the neural underpinning of aberrant behaviors in drug addiction (Volkow et al., 2013; Xie et al., 2014).

Second, our results provide insight into the “loss of control mechanism”, which is a hallmark of drug addiction and the source of its societal stigma. Quantitatively measuring the degree of control loss has proved difficult. We propose that by using neuroeconomic approaches it can be objectively quantified with “$\delta_i - \beta_i$” as an index to mark individual subjects’ self-control capacity. The balanced index (near zero) may indicate that the subject has the capacity to make a volitional decision, whereas the negative index may characterize

drug-taking and -seeking behaviors as non-volitional behaviors. The negative value of the index may define a pathological state that facilitates the activation of a metaphorical switch, thereby rendering subjects more vulnerable to relapse (Leshner, 1997).

Third, in translational practice, the imbalanced tilt between the β-δ-networks represents a pathological state and could be regarded as a functional endophenotype which not only characterizes drug abuse, but also characterizes many other disorders with aberrant behavior. This endophenotype has the potential to guide informed treatment and to monitor whether a medication targets either the β- or δ-networks, or both.

Finally, we realize that this study has several limitations. Certainly, differences between heroin addicts and nondrug-using healthy controls extend beyond the reported age and education variables. There is insufficient information to address whether the imbalanced activity between the β- and δ-networks is due to factors such as the neural effects of heroin use itself, the heroin users' lifestyles and impulse control, or other factors that might predispose an individual to heroin use. Further study will be needed to determine whether the pathological state between the β- and δ-networks is long-lasting and how it may interact with environmental and genetic factors, and different drugs of abuse (Ersche et al., 2012). Second, it should be noted that we employed global signal regression in our preprocessing procedure. We base our rationale for using this preprocessing step mainly on recent studies suggesting that the observed anticorrelation cannot be explained solely as a consequence of preprocessing using global signal regression (see supplementary text for detailed description and references). Third, when conducting voxelwise ANCOVA and linear regression anlaysis, we used both the left and the right z-maps of each individual as input, and further regressed out the effect of side' to obtain a non-lateralized result. This approach is utilized to remove the possible laterality effects between two groups.

Supplementary Material

Refer to Web version on PubMed Central for supplementary material.

Acknowledgments

The authors would like to thank Ms. Julia K. Brynildsen, B.A., Mr. Yihong Yang, Ph.D. for editorial assistance, Mr. B. Douglas Ward, MS, for discussions on the statistical analysis. This work was supported by the National Natural Science Foundation of China, No. 81271470 (ZY), AWS12J003 (ZY), 31300840 (LBW) and National Institutes of Health grant, RO1 DA10214 (SJL).

Abbreviations

3D-SPGR	three-dimensional spoiled gradient-recalled echo
ADHD	attention deficit hyperactivity disorder
AFNI	Analysis of Functional NeuroImages (software)
ANCOVA	analysis of covariance
BIS	Barratt impulsiveness scale

CC	Cross-correlation coefficient
CN	control nondrug-using
DLPFC	dorsolateral prefrontal cortex
DMPFC	dorsal medial prefrontal cortex
DSM-IV	diagnostic and statistical manual of mental disorders, 4th edition
EPI	echo planar imaging
FC	functional connectivity
FOV	field of view
FWHM	full width at half maximum
GM	gray matter
HD	heroin-dependent
iBOLD	intrinsic spontaneous blood oxygen level-dependent
IFG	inferior frontal gyrus
IPL	inferior parietal lobule
LOO	leave-one-out
MNI	Montreal Neurological Institute
NAcc	neucleus accumbens
o-VBM	Optimized Voxel-Based Morphometric
OFC	orbitofrontal cortex
PCC	posterior cingulate cortex
ROI	region of interest
SCID	structured clinical interview for DSM-IV
SPM8	Statistical Parametric Mapping, version 8 (matlab package)
TE	echo time
TR	repetition time
vmPFC	ventral medial prefrontal cortex
WM	white matter

References

Auer DP. Spontaneous low-frequency blood oxygenation level-dependent fluctuations and functional connectivity analysis of the ‘resting’ brain. Magnetic resonance imaging. 2008; 26:1055–1064. [PubMed: 18657923]

Baler RD, Volkow ND. Drug addiction: the neurobiology of disrupted self-control. Trends Mol Med. 2006; 12:559–566. [PubMed: 17070107]

Bartra O, McGuire JT, Kable JW. The valuation system: a coordinate-based meta-analysis of BOLD fMRI experiments examining neural correlates of subjective value. NeuroImage. 2013; 76:412–427. [PubMed: 23507394]

Baumgartner T, Knoch D, Hotz P, Eisenegger C, Fehr E. Dorsolateral and ventromedial prefrontal cortex orchestrate normative choice. Nat Neurosci. 2011; 14:1468–1474. [PubMed: 21964488]

Bechara A. Decision making, impulse control and loss of willpower to resist drugs: a neurocognitive perspective. Nat Neurosci. 2005; 8:1458–1463. [PubMed: 16251988]

Bickel WK, Miller ML, Yi R, Kowal BP, Lindquist DM, Pitcock JA. Behavioral and neuroeconomics of drug addiction: competing neural systems and temporal discounting processes. Drug Alcohol Depend. 2007; 90(Suppl 1):S85–91. [PubMed: 17101239]

Biswal B, Yetkin FZ, Haughton VM, Hyde JS. Functional connectivity in the motor cortex of resting human brain using echo-planar MRI. Magn Reson Med. 1995; 34:537–541. [PubMed: 8524021]

Bullmore E, Sporns O. Complex brain networks: graph theoretical analysis of structural and functional systems. Nat Rev Neurosci. 2009; 10:186–198. [PubMed: 19190637]

Dalley JW, Everitt BJ, Robbins TW. Impulsivity, compulsivity, and top-down cognitive control. Neuron. 2011; 69:680–694. [PubMed: 21338879]

Engel AK, Fries P, Singer W. Dynamic predictions: oscillations and synchrony in top-down processing. Nat Rev Neurosci. 2001; 2:704–716. [PubMed: 11584308]

Ersche KD, Jones PS, Williams GB, Turton AJ, Robbins TW, Bullmore ET. Abnormal brain structure implicated in stimulant drug addiction. Science. 2012; 335:601–604. [PubMed: 22301321]

Fair DA, Schlaggar BL, Cohen AL, Miezin FM, Dosenbach NUF, Wenger KK, Fox MD, Snyder AZ, Raichle ME, Petersen SE. A method for using blocked and event-related fMRI data to study "resting state" functional connectivity. NeuroImage. 2007; 35:396–405. [PubMed: 17239622]

Figner B, Knoch D, Johnson EJ, Krosch AR, Lisanby SH, Fehr E, Weber EU. Lateral prefrontal cortex and self-control in intertemporal choice. Nat Neurosci. 2010; 13:538–539. [PubMed: 20348919]

Fox MD, Raichle ME. Spontaneous fluctuations in brain activity observed with functional magnetic resonance imaging. Nat Rev Neurosci. 2007; 8:700–711. [PubMed: 17704812]

Fransson P. Spontaneous low-frequency BOLD signal fluctuations: An fMRI investigation of the resting-state default mode of brain function hypothesis. Hum Brain Mapp. 2005; 26:15–29. [PubMed: 15852468]

Fu LP, Bi G-h, Zou Z-t, Wang Y, Ye E-m, Ma L, Ming-Fan Yang Z. Impaired response inhibition function in abstinent heroin dependents: an fMRI study. Neurosci Lett. 2008; 438:322–326. [PubMed: 18485592]

Good CD, Johnsrude IS, Ashburner J, Henson RN, Friston KJ, Frackowiak RS. A voxel-based morphometric study of ageing in 465 normal adult human brains. NeuroImage. 2001; 14:21–36. [PubMed: 11525331]

Grabenhorst F, Grabenhorst F, Rolls ET, Rolls ET. Value, pleasure and choice in the ventral prefrontal cortex. Trends Cogn Sci (Regul Ed). 2011; 15:56–67. [PubMed: 21216655]

Grabenhorst F, Rolls E, Parris B. How the brain represents the reward value of fat in the mouth. Cerebral Cortex. 2010; 20:1082–1091. [PubMed: 19684248]

Greicius MD. Functional connectivity in the resting brain: A network analysis of the default mode hypothesis. Proceedings of the National Academy of Sciences. 2003; 100:253–258.

Gu H, Salmeron BJ, Ross TJ, Geng X, Zhan W, Stein EA, Yang Y. Mesocorticolimbic circuits are impaired in chronic cocaine users as demonstrated by resting-state functional connectivity. NeuroImage. 2010; 53:593–601. [PubMed: 20603217]

Hare TA, Camerer CF, Knoepfle DT, Rangel A. Value computations in ventral medial prefrontal cortex during charitable decision making incorporate input from regions involved in social cognition. J Neurosci. 2010; 30:583–590. [PubMed: 20071521]

Hare TA, Camerer CF, Rangel A. Self-control in decision-making involves modulation of the vmPFC valuation system. Science. 2009; 324:646–648. [PubMed: 19407204]

Kable JW, Glimcher PW. The neural correlates of subjective value during intertemporal choice. Nat Neurosci. 2007; 10:1625–1633. [PubMed: 17982449]

Kable JW, Glimcher PW. The neurobiology of decision: consensus and controversy. Neuron. 2009; 63:733–745. [PubMed: 19778504]

Lawrence AJ, Luty J, Bogdan NA, Sahakian BJ, Clark L. Impulsivity and response inhibition in alcohol dependence and problem gambling. Psychopharmacology (Berl). 2009; 207:163–172. [PubMed: 19727677]

Leshner AI. Addiction is a brain disease, and it matters. Science. 1997; 278:45–47. [PubMed: 9311924]

Li N, Ma N, Liu Y, He XS, Sun DL, Fu XM, Zhang X, Han S, Zhang DR. Resting-state functional connectivity predicts impulsivity in economic decision-making. J Neurosci. 2013; 33:4886–4895. [PubMed: 23486959]

Li SJ, Li Z, Wu G, Zhang MJ, Franczak M, Antuono PG. Alzheimer Disease: evaluation of a functional MR imaging index as a marker. Radiology. 2002; 225:253–259. [PubMed: 12355013]

Limbrick-Oldfield EH, van Holst RJ, Clark L. Fronto-striatal dysregulation in drug addiction and pathological gambling: Consistent inconsistencies? Neuroimage Clin. 2013; 2:385–393. [PubMed: 24179792]

Ma N, Liu Y, Li N, Wang CX, Zhang H, Jiang XF, Xu HS, Fu XM, Hu X, Zhang DR. Addiction related alteration in resting-state brain connectivity. NeuroImage. 2010; 49:738–744. [PubMed: 19703568]

McClure SM, Ericson KM, Laibson DI, Loewenstein G, Cohen JD. Time discounting for primary rewards. J Neurosci. 2007; 27:5796–5804. [PubMed: 17522323]

McClure SM, Laibson DI, Loewenstein G, Cohen JD. Separate neural systems value immediate and delayed monetary rewards. Science. 2004; 306:503–507. [PubMed: 15486304]

Meehan TP, Bressler SL. Neurocognitive networks: findings, models, and theory. Neurosci Biobehav Rev. 2012; 36:2232–2247. [PubMed: 22921284]

Monterosso J, Piray P. Neuroeconomics and the Study of Addiction. Biol Psychiatry. 2012; 75:107–112. [PubMed: 22520343]

Park HJ, Friston K. Structural and functional brain networks: from connections to cognition. Science. 2013; 342:1238411. [PubMed: 24179229]

Patton JH, Stanford MS, Barratt ES. Factor structure of the Barratt impulsiveness scale. J Clin Psychol. 1995; 51:768–774. [PubMed: 8778124]

Peters J, Büchel C. The neural mechanisms of inter-temporal decision-making: understanding variability. Trends Cogn Sci (Regul Ed). 2011; 15:227–239. [PubMed: 21497544]

Reuben E, Sapienza P, Zingales L. Time discounting for primary and monetary rewards. Economics Letters. 2010; 106:125–127.

Shannon BJ, Raichle ME, Snyder AZ, Fair DA, Mills KL, Zhang D, Bache K, Calhoun VD, Nigg JT, Nagel BJ, Stevens AA, Kiehl KA. Premotor functional connectivity predicts impulsivity in juvenile offenders. Proceedings of the National Academy of Sciences. 2011; 108:11241–11245.

Sharp C, Monterosso J, Montague PR. Neuroeconomics: a bridge for translational research. Biol Psychiatry. 2012; 72:87–92. [PubMed: 22727459]

Sonuga-Barke EJS, Fairchild G. Neuroeconomics of attention-deficit/hyperactivity disorder: differential influences of medial, dorsal, and ventral prefrontal brain networks on suboptimal decision making? Biol Psychiatry. 2012; 72:126–133. [PubMed: 22560046]

Steinbeis N, Bernhardt BC, Singer T. Impulse control and underlying functions of the left DLPFC mediate age-related and age-independent individual differences in strategic social behavior. Neuron. 2012; 73:1040–1051. [PubMed: 22405212]

Theodoridis, S.; Koutroumbas, K. Pattern Recognition. 3. Academic Press; San Diego, CA: 2006. Linear Classifiers.

Tomasi D, Volkow ND. Striatocortical pathway dysfunction in addiction and obesity: differences and similarities. Crit Rev Biochem Mol Biol. 2013; 48:1–19. [PubMed: 23173916]

Volkow ND, Wang GJ, Tomasi D, Baler RD. Unbalanced neuronal circuits in addiction. Curr Opin Neurobiol. 2013; 23:639–648. [PubMed: 23434063]

Volkow ND, Wang GJ, Fowler JS, Tomasi D, Baler R. Food and drug reward: overlapping circuits in human obesity and addiction. Curr Top Behav Neurosci. 2012; 11:1–24. [PubMed: 22016109]

Xie C, Li SJ, Shao Y, Fu L, Goveas J, Ye E, Li W, Cohen AD, Chen G, Zhang Z, Yang Z. Identification of hyperactive intrinsic amygdala network connectivity associated with impulsivity in abstinent heroin addicts. Behav Brain Res. 2011; 216:639–646. [PubMed: 20851718]

Xie C, Shao Y, Ma L, Zhai T, Ye E, Fu L, Bi G, Chen G, Cohen A, Li W, Chen G, Yang Z, Li SJ. Imbalanced functional link between valuation networks in abstinent heroin-dependent subjects. Mol Psychiatry. 2014; 19:10–12. [PubMed: 23207652]

Zhai TY, Shao YC, Xie CM, Ye E-m, Zou F, Fu LP, Li WJ, Chen G, Chen GY, Zhang ZG, Li SJ, Yang Z. Altered intrinsic hippocmapus declarative memory network and its association with impulsivity in abstinent heroin dependent subjects. Behav Brain Res. 2014; 272:209–217. [PubMed: 25008351]

Highlights

We characterized the nature of links between neural correlates of valuation networks.

With the link to vmPFC, δ and β networks were found jointly influence the impulsivity.

The δ and β networks were balanced and competitively control impulsivity in CN group.

The δ and β networks were imbalanced and mutually reinforce impulsivity in HD group.

This altered δ-β relationship could serve as the endophenotype of aberrant behaviors.

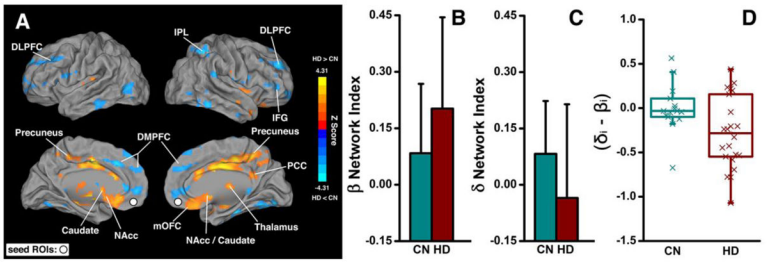

Fig. 1. Differences in vmPFC-based functional connectivity between the HD and CN groups and their numerical presentations in the β- and δ-networks

(A) Brain regions with enhanced functional connectivity (warm color) and decreased functional connectivity (cold color) in HD subjects compared with CN subjects; the white circles indicate the locations of the bilateral vmPFC as the seed ROIs. **(B)** and **(C),** Numeric representations of the map shown in **(A)** with averaged functional connectivity in the β- and δ-networks in CN and HD subjects, respectively. **(D)** The boxplot of the difference in functional connectivity strength between the δ- and β-networks in individual subjects. mOFC: medial OFC.

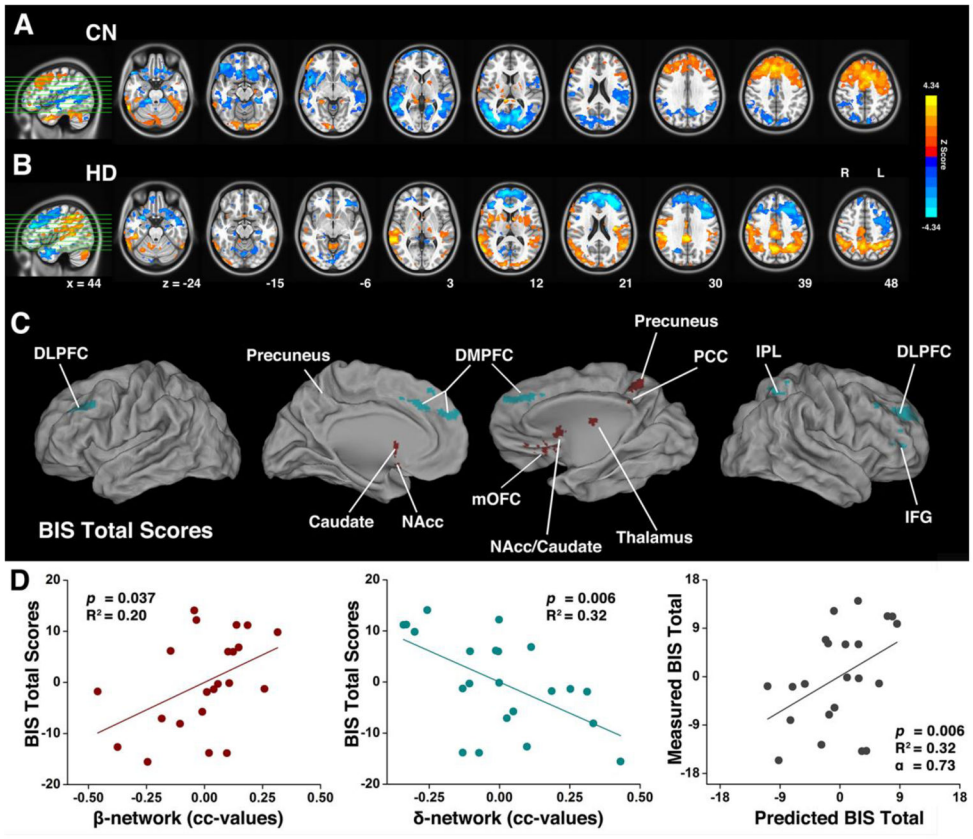

Fig. 2. The behavioral (BIS Total) significance of the imbalanced β- and δ-networks in HD subjects

The neural correlates of the BIS total score in the CN group **(A)** and the HD group (**B**). **(C)** Overlapping regions from the conjunction analysis among 1) the neural correlates of impulsivity measured with the BIS total score; 2) the difference maps in vmPFC-based functional connectivity between CN and HD groups; and 3) the predefined regions of β- and δ-networks. The red color represents the spatially segregated β-network components and the green color represents the spatially segregated δ-network components. **(D)** The two-dimensional scatterplots of the multivariate linear regression model with integrated β- and δ-network indices ($BIS=a_0+a_1\beta+a_2\delta+\varepsilon$) for HD subjects. The β-network index *positively* correlated with impulsivity (left panel) and the δ-network index *negatively* correlated with impulsivity (middle panel), measured by the BIS total score. The multivariate linear regression model was cross-validated with the LOO method (right panel).

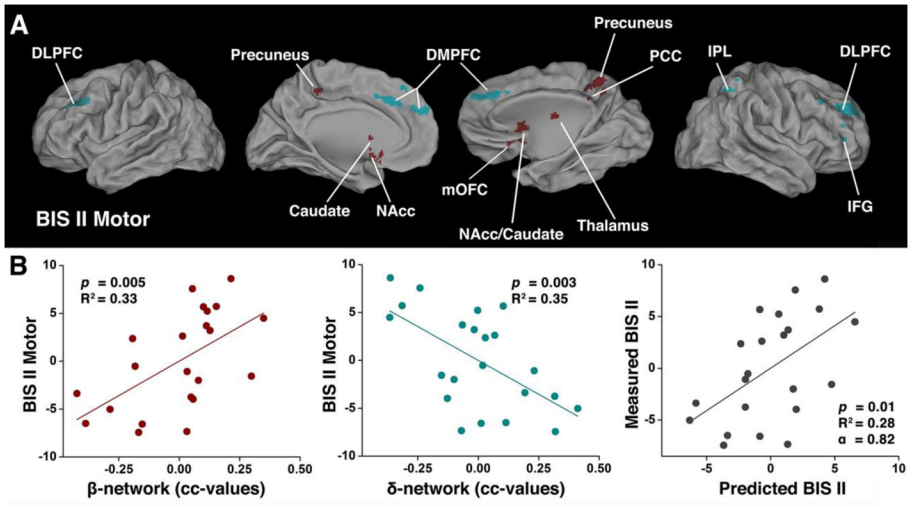

Fig. 3. The behavioral (BIS-II Motor) significance of the imbalanced β- and δ-networks in HD subjects

(A) and **(B)** are the same, as described in Figs. 2C and 2D, respectively, except that the BIS-11 Total score was replaced with the BIS-II Motor score in HD subjects.

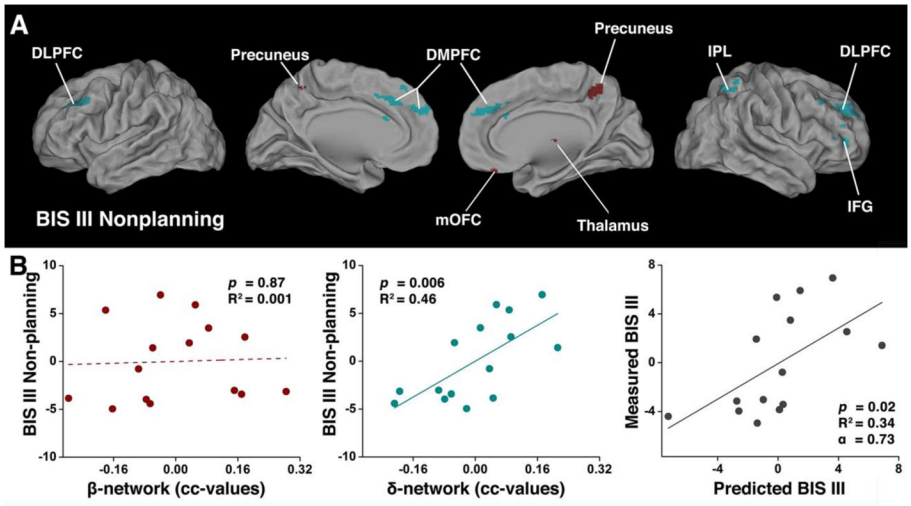

Fig. 4. The behavioral (BIS-III Nonplanning) significance of the balanced β- and δ-networks in CN subjects

(A) Overlapping regions from the conjunction analysis among 1) the neural correlates of impulsivity measured with the BIS-III Nonplanning score; 2) the difference maps in vmPFC-based functional connectivity between NC and HD groups; and 3) the predefined regions of β- and δ-networks. The red color represents the spatially segregated β-network components and the cyan color represents the spatially segregated δ-network components. (**B**) The two-dimensional scatterplots of multivariate linear regression model with integrated β- and δ-network indices ($BIS=a_0+a_1\beta+a_2\delta+\varepsilon$) for CN subjects. The β-network index did not correlate with impulsivity (left panel). In contrast, the δ-network index *positively* correlated with impulsivity (middle panel), measured by the BIS-III Nonplanning score. The multivariate linear regression model was cross-validated with the LOO method (right panel).

Table 1

Demographic information and behavioral evaluation.

	HD (n=22)	CN (n=15)	*p* value
	Mean ± SD	Mean ± SD	
Age (years)	33.05 ± 6.04	28.87 ± 8.12	0.10
Education (years)	10.86 ± 2.40	9.60 2±.16	0.10
Duration of heroin use (years)	6.59 ± 3.72	N/A	N/A
Dosage of heroin used (g/day)	0.96 ± 1.26	N/A	N/A
Abstinent period (days)	56.09 ± 17.50	N/A	N/A
BIS total score	66.45 ± 10.07	59.33 ± 6.51	0.007
BIS I Attention	18.27 ± 2.69	16.4 ± 2.82	0.03
BIS II Motor	23.09 ± 5.20	20.27 ± 2.63	0.02
BIS III Nonplanning	25.09 ± 4.21	22.67 ± 4.27	0.049
Gray matter volume (mm^3)	600.79 ± 57.94	668.28 ± 89.04	0.02

SD: standard deviation.

Table 2

The Clusters obtained from a conjunction analysis between the predefined regions in the β- and δ-networks and the neural correlates of BIS Total scores in HD and CN groups.

					Talairach Coordinates (LPI)			
		Brain Region	**Side**	**BA**	**x**	**y**	**z**	**Z Scores**
Overlapped with β-Network	**ROI 1**	**Precuneus**	L	7	−1	−45	48	2.89
	ROI 2	**Precuneus**	R	7	4	−43	47	3.43
	ROI 3	**NAcc**	L		−9	10	−9	2.62
	ROI 4	**NAcc**	R		11	11	−6	3.16
	ROI 5	**Caudate**	L		−10	7	9	2.39
	ROI 6	**Caudate**	R		11	12	−2	3.76
	ROI 7	**mOFC**	R	11	6	41	−25	3.19
	ROI 8	**Thalamus**	R		4	−13	8	3.15
	ROI 9	**PCC**	R	23	2	−40	26	2.25
Overlapped with δ-Network	**ROI 10**	**DMPFC**	L	8	−7	27	34	−3.54
	ROI 11	**DMPFC**	R	8	4	48	27	−2.78
	ROI 12	**DLPFC**	L	9	−46	33	36	−3.23
	ROI 13	**DLPFC**	R	9	43	29	43	−2.60
	ROI 14	**IFG**	R	45	39	36	6	−3.66
	ROI 15	**IPL**	R	40	41	−54	60	−3.63

BA: Brodmann area; LPI: the direction of the coordinates listed; mOFC: medial OFC.

Table 3

The Clusters obtained from a conjunction analysis between the predefined regions in the β-and δ-networks and the neural correlates of BIS-II Motor scores in HD and CN groups.

					Talairach Coordinates (LPI)			
		Brain Region	Side	BA	x	y	z	Z Scores
Overlapped with β-Network	ROI 1	Precuneus	L	7	−2	−53	49	2.61
	ROI 2	Precuneus	R	7	3	−43	47	3.43
	ROI 3	NAcc	L		−9	11	−9	3.01
	ROI 4	NAcc	R		12	13	−7	3.31
	ROI 5	Caudate	L		−11	6	10	2.37
	ROI 6	Caudate	R		11	12	−2	3.76
	ROI 7	Thalamus	R		4	−13	8	3.15
	ROI 8	PCC	R	23	5	−42	27	2.42
Overlapped with δ-Network	ROI 9	DMPFC	L	8	−7	27	34	−3.54
	ROI 10	DMPFC	R	8	4	46	27	−2.81
	ROI 11	DLPFC	L	9	−48	31	35	−3.04
	ROI 12	DLPFC	R	9	42	29	40	−2.49
	ROI 13	IFG	R	45	41	32	8	−3.69
	ROI 14	IPL	R	40	41	−54	60	−3.63

BA: Brodmann area; LPI: the direction of the coordinates listed.

Table 4

The Clusters obtained from a conjunction analysis between the predefined regions in the β-and δ-networks and the neural correlates of BIS-III Nonplanning scores in HD and CN groups.

					Talairach Coordinates (LPI)			
		Brain Region	**Side**	**BA**	**x**	**y**	**z**	**Z Scores**
Overlapped with β-Network	**ROI 1**	**Precuneus**	L	7	−1	−45	48	2.89
	ROI 2	**Precuneus**	R	7	3	−43	47	3.43
	ROI 3	**rmOFC**	R	11	6	41	−26	3.28
	ROI 4	**Thalamus**	R		7	−22	3	2.90
	ROI 5	**PCC**	R	23	8	−45	21	2.54
Overlapped with δ-Network	**ROI 6**	**DMPFC**	L	8	−7	27	34	−3.54
	ROI 7	**DMPFC**	R	8	4	46	27	−2.81
	ROI 8	**DLPFC**	L	9	−46	32	36	−3.04
	ROI 9	**DLPFC**	R	9	43	29	43	−2.60
	ROI 10	**IFG**	R	45	40	33	2	−2.81
	ROI 11	**IPL**	R	40	41	−54	60	−3.63

BA: Brodmann area; LPI: the direction of the coordinates listed; rmOFC: right medial OFC.